AIP Review of Scientific Instruments

Note: A new angle-resolved proton energy spectrometer

Y. Zheng, L. N. Su, M. Liu, B. C. Liu, Z. W. Shen et al.

Citation: Rev. Sci. Instrum. **84**, 096103 (2013); doi: 10.1063/1.4820918
View online: http://dx.doi.org/10.1063/1.4820918
View Table of Contents: http://rsi.aip.org/resource/1/RSINAK/v84/i9
Published by the AIP Publishing LLC.

REVIEW OF SCIENTIFIC INSTRUMENTS **84**, 096103 (2013)

Note: A new angle-resolved proton energy spectrometer

Y. Zheng (郑铁),[1] L. N. Su (苏鲁宁),[1] M. Liu (刘梦),[1] B. C. Liu (刘必成),[1]
Z. W. Shen (沈忠伟),[1] H. T. Fan (范海涛),[1] Y. T. Li (李玉同),[1,a)] L. M. Chen (陈黎明),[1]
X. Lu (鲁欣),[1] J. L. Ma (马景龙),[1] W. M. Wang (王伟民),[1] Z. H. Wang (王兆华),[1]
Z. Y. Wei (魏志义),[1] and J. Zhang (张杰)[1,2,b)]
[1]*Beijing National Laboratory for Condensed Matter Physics, Institute of Physics, Chinese Academy of Sciences, Beijing 100190, China*
[2]*Key Laboratory for Laser Plasmas (MoE) and Department of Physics, Shanghai Jiao Tong University, Shanghai 200240, China*

(Received 7 June 2013; accepted 25 August 2013; published online 6 September 2013)

In typical laser-driven proton acceleration experiments Thomson parabola proton spectrometers are used to measure the proton spectra with very small acceptance angle in specific directions. Stacks composed of CR-39 nuclear track detectors, imaging plates, or radiochromic films are used to measure the angular distributions of the proton beams, respectively. In this paper, a new proton spectrometer, which can measure the spectra and angular distributions simultaneously, has been designed. Proton acceleration experiments performed on the Xtreme light III laser system demonstrates that the spectrometer can give angle-resolved spectra with a large acceptance angle. This will be conductive to revealing the acceleration mechanisms, optimization, and applications of laser-driven proton beams. © *2013 AIP Publishing LLC*. [http://dx.doi.org/10.1063/1.4820918]

Laser-driven proton acceleration has been investigated for several decades[1–3] because of potential applications such as advanced imaging,[4] fast ignition,[5] cancer treatment,[6] etc. Target normal sheath acceleration (TNSA),[7] radiation pressure acceleration (RPA),[8] and other mechanisms have been proposed to accelerate protons. Protons with energy >60 MeV[9,10] have been experimentally obtained.

The main characteristics of the proton beams, such as the energy spectrum, divergence, and emission direction, are sensitive to experimental conditions. Lindau *et al.*[11] demonstrated that the proton beam gradually deviates from the target normal direction towards the laser forward direction with the enhancing of the amplified spontaneous emission (ASE) pedestal before the main laser pulse. Xu *et al.*[12] observed that spatial distribution of the proton beam was modified by the shock waves induced by strong pre-pulses. Lundh *et al.* obtained different proton spectra in different directions.[13] Comprehensive and accurate measurements of proton beams are important to understand protons generation, control and applications.

It is difficult to measure the energy and angular distributions of a proton beam simultaneously by traditional methods. In proton acceleration experiments, a Thomson parabola ion spectrometer[14] (TP) is typically used to measure spectra and stacks of CR-39 nuclear track detectors, Fujifilm imaging plates (IPs), or radiochromic films (RCFs) are used to measure angular distributions of the proton beams. The TP is a powerful device to measure the energy spectra and the charge-to-mass ratios of charged ions. Since a pinhole is typically used as an entrance, ions are only allowed to enter the spectrometer at small angle in space. Therefore, a TP with a pinhole entrance cannot give the angular distributions of proton beams. On the other hand, the stacks of particle detectors can measure angular distributions but cannot resolve spectra with high resolutions (although rough spectra can be estimated by using proton penetration depth in multilayer stacks).

We present a new proton energy spectrometer that can obtain the angular distribution and spectral information of proton beams simultaneously. Compared to the traditional TP, the entrance pinhole is replaced by a slit and only the magnetic field is retained to deflect protons. The energy range of the spectrometer is 0.6–3 MeV and resolution (ΔE/E) is better than 10% for 3 MeV protons. The angular-resolved energy distributions of proton beams have been demonstrated with the new spectrometer in a proton acceleration experiment performed on the Xtreme Light III laser system[15] at the Institute of Physics, Chinese Academy of Sciences.

A schematic view of the new spectrometer is shown in Fig. 1(a). A lead slit, instead of a pinhole, is used to collect a portion of proton beams into the spectrometer. Three slits with widths 200 μm, 300 μm, and 500 μm have been fabricated. Narrow slits give higher energy resolution, but less proton flux. In order to have a large collection angle, the slit should be as long as possible. However, it should shorter than the distance between the magnets because the change of the magnetic field is more gradual in the center. We use a 30 mm long slit for our spectrometer. The spectrometer is designed to be compact with a size of 33 cm × 13 cm × 15 cm.

A slowly varying magnetic field, which is almost parallel to the slit, is generated by a pair of 60 mm × 60 mm permanent magnets with a separation of 40 mm. The field strength at the magnetic field center is 0.3 T. Due to the long distance between the north and south poles, the magnetic field strength cannot be considered as a uniform distribution over the whole space. To obtain the relationship between the position on detector and energy of the protons, the magnetic field distribution is measured with a magnetometer. The y-component of

---

[a)] Electronic mail: ytli@aphy.iphy.ac.cn.
[b)] Electronic mail: jzhang@aphy.iphy.ac.cn.

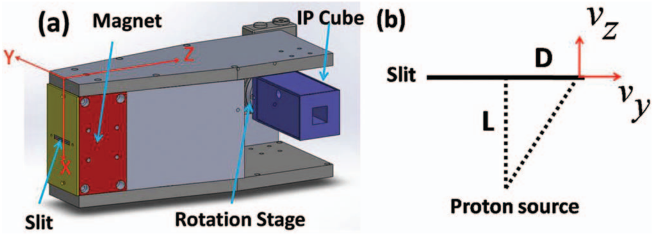

FIG. 1. (a) CAD design of the spectrometer. The magnetic field direction is oriented along the y-axis. Four image plates are equipped on the IP cube. (b) Sketch of the velocity of the protons. D is the distance from the proton position on the slit to the center of the slit and L is the distance between the source and the slit.

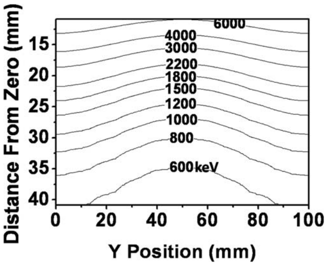

FIG. 3. The energy dispersion contours on the detection plane. The numbers in the picture represent energies of protons in the units of keV.

the magnetic field deflects protons upward and the other two component coordinates do not affect the dispersion. Therefore, only B_y is measured. Magnetic field spatial distributions in the x, y, z directions obtained by Gauss fitting are shown in Fig. 2.

Due to the use of a slit, protons come from a quasi-point source and enter the spectrometer at different incidence angles. Two components of the protons' velocities shall be considered when we calculate proton energy. v_z is calculated from the Lorentz equation while v_y is calculated from calibration. The relationship between the proton velocities v_y and v_z is given by $v_y/v_z = D/L$, where D is the horizontal distance of the proton position on the slit plane to the center of slit and L is the distance between the source and the slit, shown in Fig. 1(b).

We have developed a three-dimensional code based on the discussion above to calculate the energy dispersion corresponding to each position on the detector plane. Figure 3 gives the dispersion contours on the detected plane.

The distance between the rear edge of magnetic field and the detector, which is called drift length, is 220 mm. We chose Fujifilm imaging plates as proton recording media, because of their high sensitivity, fast readouts, and reusability. Four IPs are equipped on each side of a rotatable cube driven by a motor at the back of the spectrometer. Such a design can improve experiment efficiency because we can vent and pump down the target chamber once every four shots. The entire body of the spectrometer is wrapped in a heavy metal (normally lead) to block stray light, electrons, and x-rays to reduce noise.

The proton acceleration experiment was performed on the Xtreme light III Ti:sapphire laser system. A *p*-polarized laser pulse with an energy of 2–3 J at 800 nm in 100 fs was focused onto aluminum foil targets at an incidence angle of 15°. Different thicknesses of targets were used. The focal spot size was about 10 μm in diameter at the full width at half maximum.

The spectrometer was installed behind the target, 10 cm away from the source. This gave a collection angle of 16°, which can cover the angular range between the target normal and the laser propagation direction. A 60 μm copper wire was aligned in the target normal direction to act as a fiducial.

Only magnetic fields are applied in the spectrometer. To distinguish the protons from the other ions, a 7 μm thick aluminum filter was used to cover the IPs. The filter blocks all the carbon ions with energies <8 MeV. In our experiment, a conventional TP was also used to detect ions at the same experimental conditions and verified no carbon ions with energies >8 MeV generated under our laser conditions.

Figure 4 shows the typical raw proton images, and the angle-resolved spectra of the proton beams generated from laser interacting with 12.5 μm (a) and (c) and 4 μm (b) and (d) thick targets, respectively. For the 12.5 μm target, the proton beam is very collimated with a divergence angle as small as 3°. The peak is found to deviate from the target normal by 1° towards the laser direction. In this case, a traditional TP aligned in the target normal direction may miss the peak flux. For the 4 μm target, in Fig. 4(b), protons are spread over the entire region between the laser direction and target normal direction. Most of the high-energy (800–2000 keV) protons are emitted in the target normal direction, while low energy (600–800 keV) protons deviated in the laser direction. Significant changes in the distributions for different targets may be caused by ASE of laser. Figures 4(c) and 4(d) show the line-out spectra in the laser, target normal, and the maximum flux directions, respectively. One can see that the spectra in different directions have different energy distributions.

We have presented a new proton energy spectrometer, which can measure proton energy spectra as well as angular

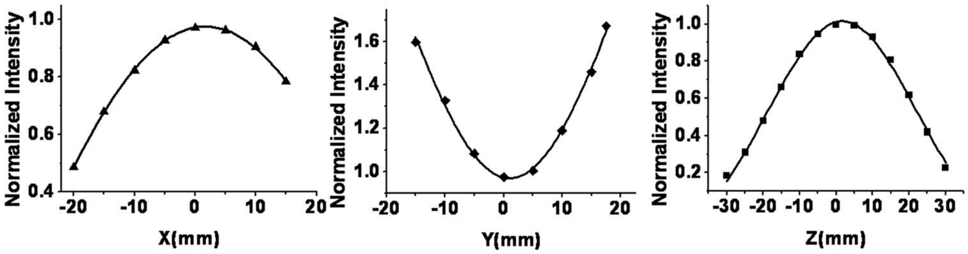

FIG. 2. Y component of magnetic field strength along three axes of the Cartesian coordinates. The discrete points are measurement results and lines are fitted by Gaussian fitting. The origin is the center of the magnetic field.

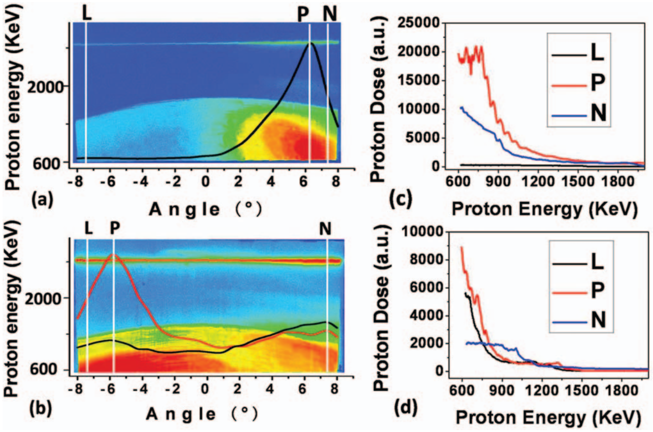

FIG. 4. The proton images on the IPs from laser interaction with 12.5 μm (a) and 4 μm (b) thick targets. The horizontal axis corresponds to the angular distribution and the vertical axis to the energy dispersion. The laser direction (L), the target normal direction (N), and the peak flux position (P) are marked. The black line in (a) shows the angular distribution of protons with integrated energies from 600 keV to 2000 keV. The red and the black lines in (b) show the angular distributions of protons with integrated energies from 600 keV to 800 keV and 800 keV to 2000 keV. (c) and (d) The line-out spectra at the three positions marked in (a) and (b), respectively.

distributions simultaneously. We experimentally verify that the spectrometer can give more information compared to the traditional Thomson parabola with a pinhole entrance, especially spatial characteristics of proton beam. The angular-resolved spectrometer can play an important role in proton beams diagnostics and will be helpful in understanding laser-induced proton generation and its applications.

This work is supported by National Basic Research Program of China (Grant No. 2013CBA01501) and National Nature Science Foundation of China (Grant Nos. 10925421, 11135012, and 10935002).

[1] G. G. Scott, J. S. Green, V. Bagnoud, C. Brabetz, C. M. Brenner, D. C. Carroll, D. A. MacLellan, A. P. L. Robinson, M. Roth, C. Spindloe, F. Wagner, B. Zielbauer, P. McKenna, and D. Neely, Appl. Phys. Lett. **101**, 024101 (2012).

[2] S. Kar, K. F. Kakolee, B. Qiao, A. Macchi, M. Cerchez, D. Doria, M. Geissler, P. McKenna, D. Neely, J. Osterholz, R. Prasad, K. Quinn, B. Ramakrishna, G. Sarri, O. Willi, X. Y. Yuan, M. Zepf, and M. Borghesi, Phys. Rev. Lett. **109**, 185006 (2012).

[3] M. H. Xu, Y. T. Li, D. C. Carroll, P. S. Foster, S. Hawkes, S. Kar, F. Liu, K. Markey, P. McKenna, M. J. V. Streeter, C. Spindloe, Z. M. Sheng, C. G. Wahlstrom, M. Zepf, J. Zheng, J. Zhang, and D. Neely, Appl. Phys. Lett. **100**, 084101 (2012).

[4] M. Borghesi, A. Schiavi, D. H. Campbell, M. G. Haines, O. Willi, A. J. MacKinnon, L. A. Gizzi, M. Galimberti, R. J. Clarke, and H. Ruhl, Plasma Phys. Controlled Fusion **43**, A267 (2001).

[5] M. Roth, T. E. Cowan, M. H. Key, S. P. Hatchett, C. Brown, W. Fountain, J. Johnson, D. M. Pennington, R. A. Snavely, S. C. Wilks, K. Yasuike, H. Ruhl, F. Pegoraro, S. V. Bulanov, E. M. Campbell, M. D. Perry, and H. Powell, Phys. Rev. Lett. **86**, 436 (2001).

[6] V. Malka, S. Fritzler, E. Lefebvre, E. d'Humieres, R. Ferrand, G. Grillon, C. Albaret, S. Meyroneinc, J. P. Chambaret, A. Antonetti, and D. Hulin, Med. Phys. **31**, 1587 (2004).

[7] S. P. Hatchett, C. G. Brown, T. E. Cowan, E. A. Henry, J. S. Johnson, M. H. Key, J. A. Koch, A. B. Langdon, B. F. Lasinski, R. W. Lee, A. J. Mackinnon, D. M. Pennington, M. D. Perry, T. W. Phillips, M. Roth, T. C. Sangster, M. S. Singh, R. A. Snavely, M. A. Stoyer, S. C. Wilks, and K. Yasuike, Phys. Plasmas **7**, 2076 (2000).

[8] A. Henig, S. Steinke, M. Schnürer, T. Sokollik, R. Hörlein, D. Kiefer, D. Jung, J. Schreiber, B. M. Hegelich, X. Q. Yan, J. Meyer-ter Vehn, T. Tajima, P. V. Nickles, W. Sandner, and D. Habs, Phys. Rev. Lett. **103**, 245003 (2009).

[9] R. A. Snavely, M. H. Key, S. P. Hatchett, T. E. Cowan, M. Roth, T. W. Phillips, M. A. Stoyer, E. A. Henry, T. C. Sangster, M. S. Singh, S. C. Wilks, A. MacKinnon, A. Offenberger, D. M. Pennington, K. Yasuike, A. B. Langdon, B. F. Lasinski, J. Johnson, M. D. Perry, and E. M. Campbell, Phys. Rev. Lett. **85**, 2945 (2000).

[10] S. A. Gaillard, T. Kluge, K. A. Flippo, M. Bussmann, B. Gall, T. Lockard, M. Geissel, D. T. Offermann, M. Schollmeier, Y. Sentoku, and T. E. Cowan, Phys. Plasmas **18**, 056710 (2011).

[11] F. Lindau, O. Lundh, A. Persson, P. McKenna, K. Osvay, D. Batani, and C. G. Wahlstrom, Phys. Rev. Lett. **95**, 175002 (2005).

[12] M. H. Xu, Y. T. Li, X. H. Yuan, Q. Z. Yu, S. J. Wang, W. Zhao, X. L. Wen, G. C. Wang, C. Y. Jiao, Y. L. He, S. G. Zhang, X. X. Wang, W. Z. Huang, Y. Q. Gu, and J. Zhang, Phys. Plasmas **13**, 104507 (2006).

[13] O. Lundh, F. Lindau, A. Persson, C. G. Wahlstrom, P. McKenna, and D. Batani, Phys. Rev. E **76**, 026404 (2007).

[14] M. Hegelich, S. Karsch, G. Pretzler, D. Habs, K. Witte, W. Guenther, M. Allen, A. Blazevic, J. Fuchs, J. C. Gauthier, M. Geissel, P. Audebert, T. Cowan, and M. Roth, Phys. Rev. Lett. **89**, 085002 (2002).

[15] Z. H. Wang, C. Liu, Z. W. Shen, Q. Zhang, H. Teng, and Z. Y. Wei, Opt. Lett. **36**, 3194 (2011).